

Exploring Prospective Benefits of Electric Vehicles for Optimal Energy Conditioning in Distribution Networks

Sasan Pirouzi¹, Jamshid Aghaei^{1,2*}, Taher Niknam¹,
Hossein Farahmand², and Magnus Korpås²

¹Department of Electrical and Electronics Engineering, Shiraz University of Technology, Shiraz, Iran

²Department of Electric Power Engineering, Norwegian University of Science and Technology (NTNU), Trondheim NO-7491, Norway

*Corresponding Author: J. Aghaei, e-mail: aghaei@sutech.ac.ir

Abstract— A potentially beneficial new opportunity is emerging around the exchange of energy between electric vehicles and the electrical energy grid, particularly as more low-carbon energy sources are connecting to the grid. Accordingly, this paper presents an optimization framework to activate the potential capabilities of electric vehicles equipped with bidirectional chargers for energy conditioning (including energy management and power quality improvement) of the future distribution networks. The proposed nonlinear optimization seeks to concurrently enhance the operation performance (using the network voltage deviation index) as well as power quality of the grid (using total harmonic distortion index). The proposed model is tested on a 33-bus distribution network to demonstrate its efficiency and performance.

Index Terms— Electric Vehicles, Energy Conditioning Management, Power Quality, Harmonic Load Flow, Non-linear Programming.

Nomenclature

Acronyms

AC	Alternating Current
AER	All-Electrical-Range
BC	Battery Capacity
BD	Benders Decomposition
CLF	Conventional Load Flow
CR	Charge Rate
DC	Direct Current
DG	Distributed Generation
ECR	Energy Consumption Requirement
EV	Electric Vehicle
FACTS	Flexible Alternating Current Transmission System
FQ	Four-Quadrant
HLF	Harmonic Load Flow
MILP	Mixed Integer Linear Programming
NLP	Non-Linear Programming
OLTC	On-Load Tap-Changers
PFC	Power Factor Correction
PHEV	Plug-in Hybrid Electric Vehicle
SOC	State of Charge
THD	Total Harmonic Distortion
UPQC	Unified Power Quality Conditioner

25

26 *Sets and indices*

b, t, l, h	Indices of bus, time, line and harmonic number
$\varphi_b, \varphi_t, \varphi_l, \varphi_h$	Sets of bus, time, line and harmonic number

27 *Variables*: All variables are in per unit (pu)

ID^p, ID^q	Active and reactive load current
IE^p, IE^q	Active and reactive current of a parking lot
IG^p, IG^q	Active and reactive current of a generation
IL^p, IL^q	Active and reactive current of a line
PB, QC	Active power of total batteries and reactive power of chargers in a parking lot
PE, QE	Active and reactive power of a parking lot
PLC, QLC	Active and reactive power loss of chargers in a parking lot
THD^v	Voltage THD [without unit]
V^r, V^i	Real and imaginary parts of voltage, respectively
V, I, S	Voltage, injecting current and apparent power, respectively

28 *Parameters*

A	Incidence matrix of lines and buses
a^p, a^q	Coefficients of active power loss of a charger
b^p, b^q	Coefficients of reactive power loss of a charger
EC	Total required energy in a parking lot in pu
GL, BL	The line conductance and susceptance in pu
HF^p, HF^q	Active and reactive harmonic factor current
IE^{max}	Charger capacity of all EVs in parking lot in pu
IG^{max}	Station or generation capacity in pu
IL^{max}	Line capacity in pu
NE_t	Number of EVs at hour t
PB^{max}	Charge rate of all batteries in a parking lot in pu
PD, QD	Active and reactive load in pu
T_{step}	Time step in hour
THD^{max}	Maximum voltage THD

V^{max}, V^{min}	Maximum and minimum voltage in pu
V_{ref}	The voltage magnitude for the reference bus in pu
29 <i>Subindexes</i>	
V, I, S	Voltage, injecting current and apparent power, respectively, in pu
Y	The network admittance matrix in pu
f_s	The fundamental frequency in hertz
W	The sub-problem objective function term
M, π	slack and dual variables in sub-problem, respectively

30

31 **1. Introduction**

32 Diesel and gasoline vehicles are one of main causes of environmental pollution and emissions. Hence,
33 Electric vehicles (EVs) are the suitable alternatives to reduce emissions. There are different types EVs
34 that can be categorized into two major categories: hybrid EVs and plug-in EVs. Hybrid EVs utilize
35 internal mechanisms to generate and store electricity, and the second type of EVs stores electricity by
36 connection to the grid. The combinations of these categories are as plug-in hybrid EVs (PHEVs) which
37 take advantage of both technologies. Commonly, PHEVs' batteries are connected to the distribution
38 network using unidirectional chargers that control active power in one direction, i.e., grid-to-vehicle
39 (G2V) [1]. Also, the unidirectional chargers use power electronic devices in their structure wherein a
40 diode full bridge is used in the first part of this charger. As a result, these chargers inject harmonic current
41 to the distribution network. In addition, EVs commonly are connected to the distribution network in the
42 peak load periods as stated in [2] and [3]. Therefore, there are two major problems due to charger structure
43 and connection time of EVs as follows: (i) increasing the energy demand while EVs are connected to the
44 network at the peak load periods [4]; (ii) injection of the harmonic current to the grid during the connection
45 of EVs to the grid [5]. According to the first problem, the network power loss, buses' voltage drop,
46 congestion of lines and energy cost will be increased in the distribution network [6]. It is also possible
47 that the bus voltage would be less than its standard minimum limit, and line power would be more than
48 its maximum standard value in the high penetration rates of EVs. In this case, system operation constraints

49 do not allow that all EVs on the network to be connected to the distribution network [7]. In other words,
50 the penetration rate of EVs should be decreased [7]. Moreover, due to the second issue, the electrical
51 equipments of distribution network would be degraded or some of the equipment would be failed [8]. For
52 instance, injection of the harmonic current to the network causes that the life time of the distribution
53 transformer is decreased as shown in [9].

54 It is noted that the energy management [10], operation planning [11] and demand side management [12]
55 are important alternatives to improve the power system indexes. In this regard, the energy management
56 of storage systems has been presented in [13]. Also, [14] and [15] express the energy management of
57 distributed generation and electrical sources, respectively. According to these researches, the energy
58 management causes improvement in network indexes such as voltage, power loss, overloading of lines and
59 network power factor. In some researches, the EVs energy management refers to the charging
60 management of EVs' batteries using an optimization framework for minimization the energy cost [16],
61 network load variation [17] and voltage deviation [18]. However, in these works, it is assumed that EVs'
62 batteries are charged in the low load period. Accordingly, the penetration of EVs could be increased, but,
63 the network indices such as the network voltage profile would not be improved at the peak load period.
64 Because, these indices are in the critical condition due to other network loads that are modeled as a
65 constant value. In this regard, [19] has used charging/discharging management of EVs batteries as the
66 EVs' energy management strategy. Based on the results of this strategy, the charging management causes
67 that EVs' batteries are charged at the low load period [20], and the network indices can be improved using
68 EVs' discharging management strategy at the critical conditions [21]. Besides, [22] and [23] have
69 presented energy management of EVs wherein the charging/discharging management of EVs' batteries,
70 and distributed generations (DGs) such as solar and wind systems have been considered concurrently.
71 Therefore, EVs' batteries can store the energy of DGs when the produced energy of the DGs is more than
72 demanded energy in the network such as low load period [22]. Also, the EVs' batteries can contribute in
73 the energy shifting programs to inject their stored energy into the network in the critical conditions, e.g.,
74 peak load hours [23]. This capability can improve the network operation indices at whole scheduling
75 periods, increase the penetration rate of EVs [24], and decrease EVs' energy cost [25]. Additionally, there

76 are other applications of EVs in the network while EVs implement the energy management strategy. For
77 instance, in [26], EVs are considered as storages in the network to be coordinated with DGs.

78 As above mentioned, the second problem refers to the injection of harmonic current into the network
79 due to nonlinear characteristics of the EVs' chargers. Different researchers such as [27], [28] and [29] in
80 the area, propose changing the structure of EVs' charger. In [27], an interleaved boost topology is used
81 in AC/DC converter or power factor correction (PFC) converter. Based on [27], the total harmonic
82 distortion (THD) of current for the new EVs' charger has been reduced. [28] and [29] propose using the
83 full bridge AC/DC converter in the charger which is called a four-quadrant (FQ) bidirectional charger.
84 This charger can be operated in four areas of the PQ power plane [28], and also it can control its harmonic
85 current [29]. Hence, the THD of the current can be reduced in this type of EVs' charger. In addition, as
86 proposed in [30], if EVs charged by group instead of individual, accordingly the current THD for the
87 group of EVs is less than the current THD for the individual EVs. It is noted that in [27]-[30], the charger
88 structure of EVs is investigated. That is, these research works have not presented the optimization problem
89 as proposed here. All in all, the taxonomy of recent works in the area is expressed in Table 1. According
90 to Table 1, three main research gaps of the available literature about the presence of EVs in the smart
91 distribution systems are as follows:

- 92 - As seen in Table 1, many works in the area, consider only active power management in the operation
93 of the distribution networks [19]-[21] while considering charging and discharging simultaneously.
94 It is noted that the continuous charging/discharging of EVs' batteries will reduce their lifetime.
- 95 - As seen in Table 1, there are limited works [27]-[30] in the area that considers the harmonic
96 compensation of EVs in the distribution networks using suitable structure of EV charger, and they
97 do not consider the harmonic compensation of other non-linear loads.
 - 98 - Finally, in the large scale networks, the calculation time is still a challenge despite using linear
99 formulations.

100 It should be noted that some researchers have used bidirectional chargers in EVs. Based on [31], the
101 bidirectional chargers include two converters that are called AC-DC bidirectional converter and DC-DC
102 bidirectional (buck and boost) converter. In the active power control mode, the AC-DC and DC-DC

103 converters are used to control the charging/discharging power of EV's battery [32]. But, AC-DC converter
104 is only needed for EVs' reactive power control [33], and EVs' harmonic current control for decreasing
105 the output current THD [34]. In these works, the metering point is the charger output point. Hence, energy
106 conditioning (power and harmonic control) should be implemented in the charger output to change power
107 and harmonic currents at this point, and the EVs' chargers do not control the network power and harmonic
108 current of the non-linear loads. In addition, references [35] and [36] have introduced different kinds of
109 custom power and FACTS devices, respectively. These devices commonly use AC-DC bidirectional
110 converter that AC side is connected to the network and DC side is connected to the energy storage device
111 such as capacitor. These devices with AC-DC bidirectional converter can control the network reactive
112 power such as D-STATCOM and UPQC, and it is capable of controlling the harmonic current of non-
113 linear loads such as active filters and D-STATCOM. Therefore, it is noted that the AC-DC bidirectional
114 converter structure of the bidirectional chargers is similar to the AC-DC converter structure of FACTS or
115 custom power devices such as D-STATCOM and active filters. Accordingly, EVs with bidirectional
116 charger can control active and reactive power of the network and compensate the harmonic current of
117 non-linear loads. Consequently, the connection point of non-linear load to the network should be
118 considered as a metering point of the charger control to decrease the current THD of the non-linear load.

119 Finally, to cope with the above three issues, an optimization approach is presented in this paper for
120 energy conditioning of the smart distribution networks and energy quality enhancement, i.e., harmonic
121 compensation of non-linear loads using EVs equipped by the bidirectional charger. At the first step, this
122 paper presents that EVs can concurrently control active (charging) and reactive power, as well as
123 harmonic current of their chargers or the distribution network. However, the active power discharging
124 mode of battery is not considered in this paper, because, it is assumed that the profit of concurrent charging
125 and discharging active power management is less than the profit of only charging management. The
126 reason is that increasing the discharging mode of EVs for injecting active power will increase
127 charging/discharging cycles that results in decreasing battery life time as well as decreasing reactive
128 power control limit. Then, the non-linear deterministic problem model is presented with the objective of
129 minimizing the voltage deviation at the fundamental frequency and the voltage THD. This objective is

130 subject to the harmonic load flow (HLF) equation, system operation limits and EVs' constraints. Finally,
 131 the Benders decomposition (BD) is used to solve the non-linear deterministic problem for increasing the
 132 calculation speed. Accordingly, to the best of authors' knowledge, the contributions of this paper with
 133 respect to the previous ones are threefold:

- 134 — Energy conditioning (simultaneous control of reactive power and harmonic current) in the smart
 135 distribution network using EVs equipped by bidirectional chargers.
- 136 — Presenting an optimization problem that models energy conditioning (including energy management
 137 and power quality improvement) of the smart distribution; the objective function of this is non-linear
 138 optimization problem is the minimization of the voltage deviation at the fundamental frequency and
 139 the voltage THD, and constraints include HLF equation, system operation limit and EVs' constraints
 140 with bidirectional chargers.
- 141 — Using the Benders Decomposition (BD) approach to accelerate the solution process of the non-linear
 142 deterministic optimization problem.

143 The rest of the paper is organized as follows: Section 2 describes the HLF and case study. The
 144 assumptions, NLP model of the deterministic problem and solution method have been presented in
 145 Section 3. Sections 4 and 5 demonstrate numerical simulations and conclusions, respectively.

146

147 **2. Case study description**

148 In this paper, the proposed problem model has been tested on the radial 33-bus distribution system [37].
 149 The loads' data are taken from [37] for the peak time, and their values have been obtained using the load
 150 percent curve, i.e., the percentage of the peak load at different times, as shown in Fig. 1 for the non-peak
 151 times. The maximum and minimum voltages for all buses are considered as 1.05 and 0.9 per unit,
 152 respectively. In addition, the non-linear load used in this paper is a 6-pulse converter that plugged into
 153 the network in buses 4, 7, 10, 13, 18, 21, 25, 27, 30 and 33 of the test case. The active and reactive
 154 harmonic factor current (HF^p , HF^q) are considered as the same, and these parameters are presented in
 155 Table 2. In addition, it is noted that the conventional load flow (CLF) is expressed for steady state
 156 conditions and linear loads. But, the waveforms of the network quantities such as bus voltage and line

157 current are not sinusoidal if non-linear loads are connected to the network. Accordingly, the non-
 158 sinusoidal waveform should be expressed as a summation of the multi sinusoidal waveforms with
 159 different magnitudes and frequencies. It should be noted that the frequency of h^{th} waveform is as $h \times f_s$
 160 wherein the f_s is the fundamental frequency of the network, and h is the harmonic order. Therefore, the
 161 harmonic load flow (HLF) is needed for implementation of the load flow in all harmonic order conditions
 162 [38] and [39]. In the HLF, the apparent power for each bus is represented as follows:

$$S_b = \sum_{h \in \phi_h} V_b^h (I_b^h)^* \quad (1)$$

163 Based on (1), there are two different presentation forms of HLP formulations as follows [38],[39]:

- 164 — In the HLP, the power components are presented only at the fundamental frequency.
- 165 — In the HLP, the power components are presented at both the fundamental frequency and harmonic
 166 frequency.

167 In the first type, the product of voltage and injecting current of a bus at the fundamental frequency is
 168 equal to the injected apparent power of the bus. In this type, the load flow at the harmonic frequency
 169 considers the relation between voltage and injected current of buses. Therefore, the HLP equations are
 170 written as follows:

$$S_b = V_b^1 (I_b^1)^* \quad (2)$$

$$I_b^h = \sum_{j \in \phi_h} Y_{b,j}^h V_j^h \quad (3)$$

171 Based on (2), the conventional load flow (CLF) is performed at the fundamental frequency for the first
 172 presentation form. Hence, the HLP includes CLF and (3) [38]. Moreover, in the second type, voltage and
 173 injected current of a bus at both fundamental frequency and harmonic frequency make the apparent power
 174 of the bus. Hence, the HLP formulation includes (1) and (3) [39]. Also, it should be noted that some of
 175 network parameters such as line reactances are changed at the harmonic frequency. Thus, the network
 176 admittance matrix would change, hence, Y^h is used in (3).

177 This paper considers three groups for EVs' number in the parking lot, and a parking lot has been
 178 assigned to each bus. The EVs' numbers are 21, 30, and 60 for the range of active load in per unit as (0,

179 0.1), (0.1, 0.2) and (0.2, >0.2), respectively. Also, the EV's characteristics are presented in Table 3. The
 180 coefficients of active power loss (a^p , a^q) and reactive power loss (b^p , b^q) of the charger, are equal to 0.09,
 181 0.0475, 0.02 and 0.02, respectively. Also, the time interval is one hour. Moreover, in this paper, two
 182 charge strategies are used as follows:

183 *Strategy I* [3], [40], [41]: The EV is connected to the network, and the EV battery is fully charged after
 184 especial charging time which is equal to BC/CR , wherein BC and CR are battery capacity and charge rate
 185 of EV, respectively. Also, the active power of total batteries in the parking lot (PB) at time t is equal to
 186 the charge rate of all batteries in parking lot (PB^{max}) at time t ($PB_{b,t} = PB_{b,t}^{max}$), where $PB_{b,t}^{max}$ is equal to
 187 $\sum_{i=1}^{NE_t} CR_i$, and NE_t is the number of EVs at hour t . Moreover, the number of EVs at each hour has been
 188 shown in the Fig. 2 (a) that is obtained based on the assumption that "EVs are connected into the
 189 distribution network when they arrive at home after their last trip" [3].

190 *Strategy II* [41]-[43]: the EV battery is not charged after its connection to the network. But, it is charged
 191 based on objective function which is introduced in the main problem. Also, the inequality of $PB_{b,t} \leq PB_{b,t}^{max}$
 192 is used in this strategy. Moreover, the number of EVs at each hour has been shown in Fig. 2 (b) that is
 193 obtained based on assumption that "EVs are connected into the distribution network when they arrive at
 194 home after their last trip" [3].

195

196 3. Mathematical formulation

197 3.1. Assumptions

198 In this section, the assumptions of the proposed problem model have been presented as follows:

- 199 1- The first type of HLP equation is used in the proposed model.
- 200 2- This paper investigates EVs' capability for energy conditioning of smart distribution networks
 201 (including network energy management and harmonic compensation of non-linear loads). Hence,
 202 the other power controlling equipment such as capacitor bank, distributed generations, OLTC are
 203 not considered.

204 3- According to [34], increasing the number of charging/discharging cycles of the EV's battery
 205 causes decreasing its lifetime. Therefore, the active power discharging mode of EV's battery is
 206 not considered. It is noted that usually the active power discharging of EVs is used in peak load
 207 times. Accordingly, it is expected that EVs would be charged in two periods, i.e., before and after
 208 peak load times. Indeed, EVs will be charged in the period of before peak load times to be
 209 discharged in the peak load times, and they are charged in the period of after peak load times to
 210 provide EVs' energy consumption requirements. According to this mechanism, the number of
 211 charging/discharging cycles of the EVs' batteries will be increased; accordingly, it will decrease
 212 their lifetime as mentioned in [34] and will decrease the charging cost. Also, the injected active
 213 power to the grid during the high price hours causes that the injection/absorption of reactive power
 214 into/from the grid to be decreased. Indeed, the discharging mode of active power will limit the
 215 reactive power control by EVs. Finally, it would be shown in simulation results that the profit of
 216 concurrent charging and discharging modes of active power management is less than the profit of
 217 just charging management.

218 4- The battery of EVs are recharged in the parking lot or parking of an apartment.

219 5- EVs are connected into the distribution network when they arrive at home after their last trip.

220 3.2. Problem formulation

221 In this section, the NLP deterministic optimization model of the energy conditioning (energy
 222 management of smart distribution network and energy quality enhancement, i.e., harmonic compensation
 223 of non-linear loads using EVs with bidirectional charger) is presented. The objective function of the
 224 proposed optimization problem includes the minimization of both the voltage deviation at the
 225 fundamental frequency and voltage THD subject to the HLP equations, system operation limits and EVs
 226 constraints.

227 *Objective function:* the objective function of the proposed problem is represented in (4). The first term
 228 of this equation refers to the minimization of voltage deviation at the fundamental frequency. Also, the
 229 minimization of the voltage THD is presented in second term of (4). It should be noted that these terms

230 are included in the objective function to investigate EVs capability to regulate voltage of buses and
 231 harmonic compensation of non-linear loads and motivate EVs for energy conditioning (energy
 232 management and harmonic current control).

$$\min \sum_{r^r, i^i} \sum_{b \in \varphi_h, t \in \varphi_t} \left\{ \frac{\sqrt{(V_{b,t,1}^r)^2 + (V_{b,t,1}^i)^2} - V_{ref}}{V_{ref}} + THD_{b,t}^v \right\} \quad (4)$$

233 It should be noted that voltage is defined as $\sqrt{\sum_{h \in \varphi_h} (V_{b,t,h}^r)^2 + (V_{b,t,h}^i)^2}$ in the harmonic space. But, based on
 234 this term, the voltage at harmonic frequency may be increased, and the voltage at fundamental frequency
 235 is reduced. Accordingly, in addition to the first term, the voltage THD is augmented in the objective
 236 function. Because, based on (3), the harmonic of current is decreased if voltage harmonic is reduced.
 237 Thus, this is the main reason that the term of current THD is not considered in this formulation.

238 *The HLP constraints:* these constraints are presented as follows based on assumption 1:

$$IG_{b,t,h}^p - ID_{b,t,h}^p - IE_{b,t,h}^p = \sum_{l \in \varphi_l} A_{l,b} IL_{l,t,h}^p \quad \forall b,t,h \quad (5)$$

$$IG_{b,t,h}^q - ID_{b,t,h}^q - IE_{b,t,h}^q = \sum_{l \in \varphi_l} A_{l,b} IL_{l,t,h}^q \quad \forall b,t,h \quad (6)$$

$$IL_{b,t,h}^p = \sum_{j \in \varphi_h} A_{l,j} \left\{ GL_{l,h} V_{b,t,h}^r - BL_{l,h} V_{b,t,h}^i \right\} \quad \forall l,t,h \quad (7)$$

$$IL_{b,t,h}^q = \sum_{j \in \varphi_h} A_{l,j} \left\{ GL_{l,h} V_{b,t,h}^i + BL_{l,h} V_{b,t,h}^r \right\} \quad \forall l,t,h \quad (8)$$

239 Equations (5) and (6) represent active and reactive current balance, respectively. Also, the active and
 240 reactive current flow of lines are defined in (7) and (8), respectively. These equations are expressed for
 241 each bus and each harmonic order at hour t . In these constraints, the value of IG^p and IG^q in all buses
 242 except the substation bus of the network is equal to zero based on assumption 2. In addition, $A_{l,b}$ is equal
 243 to 1, if the current of line l exits from bus b , and $A_{l,b}$ is equal to -1 if the current of line l enters to bus b ,
 244 otherwise, it is zero.

245 *Load constraints:* generally, the active and reactive power of load are pre-specified, and the harmonic
 246 current of load is defined as the percent of load current at the fundamental frequency. Hence, load
 247 constraints can be written as follows based on assumption 1:

$$PD_{b,t} = V_{b,t,h}^r ID_{b,t,h}^p + V_{b,t,h}^i ID_{b,t,h}^q \quad \forall b,t,h=1 \quad (9)$$

$$QD_{b,t} = V_{b,t,h}^i ID_{b,t,h}^p - V_{b,t,h}^r ID_{b,t,h}^q \quad \forall b,t,h=1 \quad (10)$$

$$ID_{b,t,h}^p = HF_{b,h}^p ID_{b,t,1}^p \quad \forall b,t,h \neq 1 \quad (11)$$

$$ID_{b,t,h}^q = HF_{b,h}^q ID_{b,t,1}^q \quad \forall b,t,h \neq 1 \quad (12)$$

248 Equations (9) and (10) are expressed based on the first type of HLP presentation. In other words, the
 249 voltage and current of the load at the fundamental frequency perform active and reactive power of the
 250 load. The relations of active and reactive load currents have been introduced in (11) and (12), respectively.

251 *Constraints of EVs/parking lots:* In this paper it is considered that there is a parking lot in each bus,
 252 and also, the active and reactive power of parking lot have been denoted by PE and QE , respectively.

253 Accordingly, we have: $PE_b + jQE_b = V_b (IE_b)^*$, $V_b = V_b^r + jV_b^i$ and $(IE_b)^* = IE_b^p - jIE_b^q$. Therefore,
 254 according to the above formulations, the equations (13) and (14) are obtained.

$$PE_{b,t} = V_{b,t,h}^r IE_{b,t,h}^p + V_{b,t,h}^i IE_{b,t,h}^q \quad \forall b,t,h=1 \quad (13)$$

$$QE_{b,t} = V_{b,t,h}^i IE_{b,t,h}^p - V_{b,t,h}^r IE_{b,t,h}^q \quad \forall b,t,h=1 \quad (14)$$

255 Moreover, the active power source in the parking lot is the total batteries of EVs which is denoted by PB .
 256 Also, this source is connected to the network though the chargers of EVs. Therefore, the PE is equal to
 257 the summation of PB and active power loss of EVs' chargers, i.e., $PLC_{b,t}$, as shown in (15).

$$PE_{b,t} = PB_{b,t} + PLC_{b,t} \quad \forall b,t \quad (15)$$

258 Also, there is an inductance in the output of the charger and it consumes reactive power that is called
 259 reactive power loss. Besides, the reactive power source in the parking lot is EVs' chargers. In the proposed
 260 problem, QC represents the reactive power of this source. Therefore, QE is equal to the summation of QC
 261 and reactive power loss of EVs' chargers, i.e., $PLC_{b,t}$, as formulated in (16).

$$QE_{b,t} = QC_{b,t} + QLC_{b,t} \quad \forall b,t \quad (16)$$

262 The active and reactive power losses of EVs' chargers depend on PE and QE as shown in equations (17)
263 and (18) [41].

$$PLC_{b,t} = a^p (PE_{b,t})^2 + a^q (QE_{b,t})^2 \quad \forall b,t \quad (17)$$

$$QLC_{b,t} = b^p (PE_{b,t})^2 + b^q (QE_{b,t})^2 \quad \forall b,t \quad (18)$$

264 In this paper, the discharging mode of the active power for EV's battery is not considered, hence, the
265 lower limit of PB is equal to zero based on the assumption 3.

$$0 \leq PB_{b,t} \leq PB_{b,t}^{\max} \quad \forall b,t \quad (19)$$

266 Where this equation is used for Strategy II, and also, it is expressed by $PB_{b,t} = PB_{b,t}^{\max}$ in Strategy I.

267 In addition, this paper assumes that EVs are plugged into the network after their daily trip based on [3],
268 hence, EVs are charged to provide their energy consumption requirements (ECRs) once per day after their
269 last trip. Also, the ECR of an EV is equal to $(1-SOC) \times BC$, which SOC and BC indicate the state of charge
270 and battery capacity, respectively. The SOC is defined as the percentage of energy remaining in the EV's
271 battery [3]. That is, the SOC is the percentage of remaining energy of EV's battery when EV arrives at
272 the parking lot after its daily trips. Hence, the SOC depends on the distance that EV derives in the electric
273 mode (L) and it is expressed as $(1-L/AER)$, where, AER , i.e., all-electrical-range, presents the total
274 distance that EV derives in the electric mode based on its battery capacity. Consequently, based on
275 assumptions 4 and 5, in (20), the EC refers to the summation of the ECR of all EVs in the parking lot.

$$\sum_{t \in \varphi_t} T_{step} PB_{b,t} = EC_b \quad \forall b \quad (20)$$

276 Finally, the capacity of EVs' chargers is limited in equation (21).

$$\sum_{h \in \varphi_h} \left\{ (IE_{b,t,h}^p)^2 + (IE_{b,t,h}^q)^2 \right\} \leq (IE_{b,t}^{\max})^2 \quad \forall b,t \quad (21)$$

277 *Constraints of harmonic indices:* there are different harmonic indices to investigate the harmonic
278 impacts in the network [37]. One of the important harmonic indices is THD that can be calculated for

279 voltage and current. But, this paper implements THD for voltage of all buses, because, the current depends
 280 to voltage. Thus, the calculation of current THD is not needed. These constraints are presented as follows:

$$THD_{b,t}^v = \sqrt{\frac{\sum_{h \in \varphi_b, h \neq 1} \left\{ (V_{b,t,h}^r)^2 + (V_{b,t,h}^i)^2 \right\}}{(V_{b,t,1}^r)^2 + (V_{b,t,1}^i)^2}} \quad \forall b, t \quad (22)$$

$$THD_{b,t}^v \leq THD_b^{\max} \quad \forall b, t \quad (23)$$

281 The voltage THD is calculated based on (22). Equation (23) limits the voltage's THD with a maximum
 282 value of THD^{\max} , which is equal to 5% based on IEEE 519 standard [44].

283 *System operation limits:* these limits include voltage bus, line current and station (generation) current
 284 limits that are presented in (24), (25) and (26), respectively.

$$(V_b^{\min})^2 \leq \sum_{h \in \varphi_b} \left\{ (V_{b,t,h}^r)^2 + (V_{b,t,h}^i)^2 \right\} \leq (V_b^{\max})^2 \quad \forall b, t \quad (24)$$

$$\sum_{h \in \varphi_l} \left\{ (IL_{l,t,h}^p)^2 + (IL_{l,t,h}^q)^2 \right\} \leq (IL_l^{\max})^2 \quad \forall l, t \quad (25)$$

$$\sum_{h \in \varphi_b} \left\{ (IG_{b,t,h}^p)^2 + (IG_{b,t,h}^q)^2 \right\} \leq (IG_b^{\max})^2 \quad \forall b, t \quad (26)$$

285 In this model, PB , QC , IE^p and IE^q are decision variables, and V^r , V^i and THD^v are the output variables
 286 of the problem.

287 3.3. Solution method

288 Constraints of system operation limits in the proposed deterministic model, i.e. (24)-(26), are the most
 289 complicated constraints. Hence, the calculation speed may be reduced. Consequently, based on [45], the
 290 BD algorithm is used to solve the proposed problem model. Generally, BD algorithm is deployed for
 291 solving the multi-stage MILP problems. But also, this algorithm can be applied to single or multi-stage
 292 NLP problems that have complicating constraints/variables in order to accelerate the calculation speed
 293 [45]. The BD algorithm includes two parts that are called master problem and sub-problem. The master
 294 problem refers to the main part of the fundamental problem, and sub-problem checks the complicating
 295 constraints using output results of the master problem. In other words, the master problem equations are
 296 (4)-(23), and the sub-problem equations can be written as follows:

$$\min_W \quad W = \sum M \quad (27)$$

297 **Subject to:**

$$\sum_{h \in \varphi_a} \left\{ (V_{b,t,h}^r)^2 + (V_{b,t,h}^i)^2 \right\} - M_{b,t,1} \leq (V_b^{\max})^2 : \pi_{b,t,1} \quad \forall b, t \quad (28)$$

$$\sum_{h \in \varphi_a} \left\{ (V_{b,t,h}^r)^2 + (V_{b,t,h}^i)^2 \right\} + M_{b,t,2} \geq (V_b^{\min})^2 : \pi_{b,t,2} \quad \forall b, t \quad (29)$$

$$\sum_{h \in \varphi_a} \left\{ (IL_{l,t,h}^p)^2 + (IL_{l,t,h}^q)^2 \right\} - M_{l,t,3} \leq (IL_l^{\max})^2 : \pi_{l,t,3} \quad \forall l, t \quad (30)$$

$$\sum_{h \in \varphi_a} \left\{ (IG_{b,t,h}^p)^2 + (IG_{b,t,h}^q)^2 \right\} - M_{b,t,4} \leq (IG_b^{\max})^2 : \pi_{b,t,4} \quad \forall b, t \quad (31)$$

$$M \geq 0 \quad (32)$$

298 Equations (28)-(32) refer to the sub-problem part of BD algorithm. It is noted that the constraints of the
 299 system operation limits part in the proposed deterministic model, i.e., (24)-(26), are the most complicated
 300 constraints. Hence, the problem of (4)-(26) can be solved hardly. For the sake of simplification, the BD
 301 algorithm is used at two parts. In the first part, the problem of (4)-(23) is solved that called master problem.
 302 The second part, called sub-problem, will check the satisfaction of equations (24)-(26) according to the
 303 solution of the master problem. To this end, the slack variable of M is added to equations (24)-(26) as
 304 equations (28)-(31). If $M > 0$, the equations (24)-(26) would not be satisfied. But, if $M = 0$, the equations
 305 (24)-(26) will be satisfied.

306 In the above formulations, M and π are slack and dual variables, respectively. Hence, the proposed
 307 problem (4)-(26) is converged if $|W| \leq \varepsilon$ (where ε is BD convergence tolerance level), otherwise ($|W| \geq \varepsilon$),
 308 the Benders cut is added to the master problem which is formulated as follows [45]:

$$\sum_{b \in \varphi_a} \left\{ \begin{array}{l} \sum_{t \in \varphi_t} \pi_{b,t,1} \left((V_b^{\max})^2 - \sum_{h \in \varphi_a} \left\{ (V_{b,t,h}^r)^2 + (V_{b,t,h}^i)^2 \right\} \right) \\ + \pi_{b,t,2} \left(\sum_{h \in \varphi_a} \left\{ (V_{b,t,h}^r)^2 + (V_{b,t,h}^i)^2 \right\} - (V_b^{\min})^2 \right) \\ + \pi_{b,t,4} \left((IG_b^{\max})^2 - \sum_{h \in \varphi_a} \left\{ (IG_{b,t,h}^p)^2 + (IG_{b,t,h}^q)^2 \right\} \right) \end{array} \right\} + \sum_{l \in \varphi_l} \sum_{t \in \varphi_t} \pi_{l,t,3} \left((IL_l^{\max})^2 - \sum_{h \in \varphi_a} \left\{ (IL_{l,t,h}^p)^2 + (IL_{l,t,h}^q)^2 \right\} \right) \leq 0 \quad (33)$$

309 The flowchart of implementing BD for the proposed problem is shown in Fig. 3.

311 4. Numerical results and discussion

312 The proposed problem model is programmed in GAMS 23.5.2 and solved using the CONOPT 3.0 solver
313 [46]. Also, it is noted that the start time for the simulation studies is 10:00 A.M due to constraints in (20).

314 1) *The impacts of EVs on the distribution network with reactive power management and harmonic*
315 *compensation*: the results of this section are shown in Fig. 4. In this study, three cases have been
316 performed as follows:

- 317 • *Case I*: Base load case that shows the results of the problem model without considering EVs in the
318 network.
- 319 • *Case II*: Distribution network operation without using EVs active and reactive power as well as
320 harmonic current control capability, and using Strategy I to charge 21% of EVs' batteries.
- 321 • *Case III*: Distribution network operation using only EVs reactive power and harmonic current control
322 capability, and using Strategy I to charge 21% of EVs' batteries.

323 In the case II, 21% of EVs are connected to the network and the power management and harmonic
324 compensation are not considered. In this case, EVs are plugged into the network after their last trip and
325 charged fully after their special charging time. Thus, the EVs do not have any impacts on the distribution
326 network after their especial charging time. Case III (21% EVs) implements the reactive power
327 management and harmonic compensation when EVs charge their battery in the distribution network. The
328 power variation between the cases I and II indicates that EVs are charged during 15:00 to 2:00 of the next
329 day as shown in Fig. 4 (a). Based on this figure, the power demand of EVs from the distribution network
330 is high in the peak load times. Hence, the voltage of all buses are leveled off with respect to the case I in
331 this period, (see Fig. 4 (b)). In this condition, the system operation limits, i.e., (24)-(26), do not allow the
332 large number of EVs to be plugged into the network. This matter has been shown in Fig. 4 (a). The voltage
333 THD of the system has been shown in Fig. 4 (c). Based on this figure, the voltage's THD of all buses in
334 the case II is larger than the voltage' THD of all buses in the case I, but, this difference is low. Case III
335 adds the reactive power management and harmonic compensation to the case II. Based on Fig. 4, the
336 power demand from the upstream network is reduced with respect to the case I. This reduction is due to

337 the injection of the reactive power to the distribution network and non-linear harmonic compensation
 338 using EVs. This is because the active power demand of loads and EVs are the same as the case II. Also,
 339 the injection of the reactive power to the network causes to increase voltage of buses with respect to the
 340 case I. In addition, the voltage THD of 17 buses is more than 5% in cases I and II, but, the voltage THD
 341 of all buses is less than 5% in case III. Also, the voltage profile and voltage THD have been improved
 342 during the peak load periods for the case III, because the reactive power management and harmonic
 343 compensation have been implemented during hours 15:00 to 2:00 of the next day as can be inferred in
 344 Fig. 4 (a). As a last note, the apparent power of the upstream network at peak load period (hour 20) for
 345 the cases II and III are 4.84 per units and 5 per units, respectively. Thus, the reactive power management
 346 and harmonic compensation of EVs in the case III causes that the apparent power of the upstream network
 347 to be reduced with respect to the case II. This reduction is 0.16 per unit or $3.2\% = 100 \cdot (5 - 4.84) / 5$. Hence,
 348 this reduction leads to more loads or EVs be able to demand power from the network.

349 *2) The impacts of EVs on the distribution network using power management and harmonic*
 350 *compensation:* In this study, three cases have been performed as follows:

- 351 • *Case I:* Base load case that shows the results of problem model without considering EVs in the
 352 network.
- 353 • *Case II:* Distribution network operation using only EVs' active power control capability, and using
 354 Strategy II to charge 100% of EVs' batteries.
- 355 • *Case III:* Distribution network operation using EVs concurrent active and reactive power as well as
 356 harmonic current control capability, and using Strategy II to charge 100% of EVs' battery.

357 Fig. 5 shows the daily pattern of the network apparent power, daily voltage profile and daily pattern of
 358 voltage THD for the bus 18. It is noted that based on Fig. 4 (b) and (c), the voltage of the bus 18 is less
 359 than all other buses' voltages, and voltage THD of the bus 18 is greater than all other buses' voltage THD;
 360 therefore, in this paper, the bus 18 is selected for the investigation of the network voltage and voltage
 361 THD for different cases. The results of the base load (no EVs) are expressed in case I, and active power
 362 management (charging management of EVs battery) only is implemented in case II (100% of EVs are

363 connected to the network). The power management and harmonic compensation using EVs are studied in
 364 the case III with 100% of EVs plugged. Based on Fig. 5 (a), the power variations between cases I and II
 365 indicate charging of EVs' batteries in the period of 23:00 to 9:00 of the next day, and EVs do not demand
 366 power from the upstream network at the other times. Hence, the voltage and voltage THD of the bus 18
 367 (or other buses) are changed in this period with respect to the case I, but, the changes of voltage THD are
 368 low. It should be noted that the penetration rate of EVs is increased to 100% in the case II, but, the network
 369 indices such as the voltage of buses, line power flow and voltage THD of buses are not improved at all
 370 times or peak load times. As stated, case III adds the reactive power management and harmonic
 371 compensation to the case II. Based on Fig. 5 (a), the apparent power of the upstream network is reduced
 372 in the period of 12:00 to 21:00 with respect to the case I, and it is increased in the period of 22:00 to 8:00
 373 of the next day with respect to the case I. The reduction of network apparent power is due to the injection
 374 of reactive power into the network as well as non-linear harmonic compensation by EVs. Indeed, in this
 375 condition, the injection of the reactive power of EVs is greater than the network reactive load. Also, the
 376 reasons of the increment of the network apparent power are: (i) the charge of active power of EVs'
 377 batteries, (ii) the injection of the reactive power of EVs' charger which is more than the network reactive
 378 load (it is more than two times of network's reactive load), and (iii) the harmonic compensation by EVs
 379 such that the employed capacity of the harmonic compensation is less than other factors. Besides, the
 380 voltage deviation of bus 18 (and other buses) is low as shown in Fig. 5 (b). In other words, the minimum
 381 voltage of the bus 18 is 0.947 per unit that indicates EVs are capable to regulate voltage of buses. Also,
 382 the voltage THD has been improved at all times for case III based on Fig. 5 (c). Because, the maximum
 383 voltage THD of the bus 18 is equal to 4.43% that is less than 5%. This shows the EVs' capability for
 384 compensation of non-linear load harmonic at all times.

385 3) *Benefits of using BD algorithm to solve the proposed problem model:* in this section, the calculation
 386 time of solving the proposed problem model with and without BD algorithm has been presented. To better
 387 show the capability of BD, three distribution networks, i.e., 33-bus, 69-bus [47] and 123-bus [48], are
 388 used. The data of non-linear loads' (6-pulse converter) connection is presented in Table 4. The other data
 389 of the problem, i.e., voltage limit, HF^p and HF^q , and EVs' data, for 69-bus and 123-bus networks is the

390 same with the previous data in section 2. Table 5 shows the calculation time of solving the proposed
391 problem model with and without BD algorithm. In this table, different solvers of GAMS software are
392 used to solve the proposed problem without BD algorithm. As seen in the table, the results of GAMS
393 solvers are the same. Based on this table, solving the proposed NLP deterministic problem model without
394 BD algorithm can be performed on small size distribution network. In other words, solving problem
395 without BD algorithm cannot find the optimal or locally optimal solutions in the large size distribution
396 networks. Also, the calculation time still is high for the small size of the distribution networks. But,
397 implementing BD algorithm would reduce the calculation time, and it can reach the global/local optimal
398 solutions in the large size of the distribution networks. In addition, the BD convergence time for the
399 proposed problem is low. In addition, table 6 shows the number of equations and variables for the problem
400 with and without BD algorithm. Based on this table, the number of equations and variables in the problem
401 without BD algorithm is less than the problem with BD algorithm. However, the calculation time of BD
402 algorithm is less than the problem without BD algorithm.

403

404 **5. Conclusions**

405 This paper proposed the energy conditioning management of the smart distribution network and energy
406 quality enhancement, i.e., harmonic compensation of non-linear loads using EVs equipped by
407 bidirectional chargers. The proposed non-linear deterministic model considers the voltage deviation at
408 the fundamental frequency and the voltage THD as the objective function, while harmonic load flow
409 equations, system operation limit, harmonic index equations and EVs constraints have been modeled as
410 optimization problem constraints. Finally, the BD algorithm is used for solving the proposed problem
411 model. Using BD algorithm to solve the optimization problem causes reduction of the calculation time
412 by 8. Based on the numerical results, the network and harmonic indices have been improved at the peak
413 load conditions if only reactive power management and harmonic compensation are implemented. Also,
414 the penetration rate of EVs would be increased to 100% if only the charging active power management is
415 used. But, the voltage deviation at the fundamental frequency and voltage THD of all buses are reduced

416 by about 48 and 51 percent, respectively, at all times of the study period in the case of the higher EVs
417 penetration rates (when EVs control the charging of active power and reactive power and compensate the
418 non-linear load harmonics). These points refer to advantages of using EVs with bidirectional chargers to
419 enable active and reactive power control capability in distribution network and compensating the
420 harmonic of non-linear loads. All in all, the main significance of the proposed energy quantity and quality
421 management services for distribution networks in the presence of EVs is that not only it will remedy the
422 challenge of increased demand due to charging EVs in the distribution network, but also, will add new
423 capabilities to manage the operation of the distribution networks proactively. Finally, the research work
424 is underway to utilize the EVs' capability in harmonic compensation of the network in addition to active
425 and reactive power management while considering the cost and revenue of this strategy for EVs.

427 **References**

- 428 [1] M.C. Kisacikoglu, Vehicle-to-Grid reactive power operation analysis of the EV/PHEV bidirectional
429 battery charger, *University of Tennessee*, 2013.
- 430 [2] B. Tarroja, L. Zhang, V. Wifvat, B. Shaffer, S. Samuelsen, "Assessing the stationary energy storage
431 equivalency of vehicle-to-grid charging battery electric vehicles," *Energy*, vol. 115, pp. 673-690, July
432 2016.
- 433 [3] S. Shafiee, M. Fotuhi-Firuzabad, and M. Rastegar, "Investigating the impacts of plug-in hybrid
434 electric vehicles on power distribution systems," *IEEE Trans. Smart Grid.*, vol. 4, no. 3, pp. 1351-
435 1360, 2013.
- 436 [4] C. Weiller, and A. Neely, "Using electric vehicles for energy services: Industry perspectives,"
437 *Energy*, vol. 77, pp. 194-200, Dec. 2014.
- 438 [5] Y. Zhao, O. Tatari, "A hybrid life cycle assessment of the vehicle-to-grid application in light duty
439 commercial fleet," *Energy*, vol. 93, pp. 1277-1286, Dec. 2015.
- 440 [6] M.S. El-Nozahy, and M.M.A. Salama, "A comprehensive study of the impacts of PHEVs on
441 residential distribution networks," *IEEE Transactions on Sustainable Energy*, vol.5, no.1, pp.332-
442 342, 2014.

- 443 [7] P. García-Triviño, J. P. Torreglosa, L. M. Fernández-Ramírez, F. Jurado, “Control and operation of
444 power sources in a medium-voltage direct-current microgrid for an electric vehicle fast charging
445 station with a photovoltaic and a battery energy storage system,” *Energy*, vol. 115, pp. 38-48, Nov.
446 2016.
- 447 [8] C. Jiang, R. Torquato, D. Salles, and W. Xu, “Method to assess the power quality impact of plug- in
448 hybrid electric vehicles,” *IEEE Transactions on Power Delivery*, vol. 29, no. 4, pp. 958- 965, 2014.
- 449 [9] J.C. Gomez, and M.M. Morcos, “Impact of EV battery chargers on the power quality of distribution
450 system”, *IEEE Transaction on Power Delivery*, vol. 18, no. 3, pp. 975- 981, 2003.
- 451 [10] E.D. Mehleri, H. Sarimveis, N.C. Markatos, and L.G. Papageorgiou, “A mathematical
452 programming approach for optimal design of distributed energy systems at the neighbourhood level,”
453 *Energy*, vol. 44, pp. 96-104, 2012.
- 454 [11] D. Zhang, N. Shah, and L.G. Papageorgiou, “Efficient energy consumption and operation
455 management in a smart building with microgrid,” *Energy Conversion and Management*, vol. 74, pp.
456 209-222, 2013.
- 457 [12] J. Silvente, A.M. Aguirre, M.A. Zamarripa, C.A. Méndez, M. Graells, and A. Espuña, “Improved
458 time representation model for the simultaneous energy supply and demand management in
459 microgrids,” *Energy*, vol. 87, pp. 615-627, 2015.
- 460 [13] S. Samsatli, and N.J. Samsatli, “A general spatio-temporal model of energy systems with a
461 detailed account of transport and storage,” *Computers & Chemical Engineering*, pp. 155-176, 2015.
- 462 [14] J. Jurasz, B. Ciapała, “Integrating photovoltaics into energy systems by using a run-off-river power
463 plant with pondage to smooth energy exchange with the power grid,” *Applied Energy*, vol. 198, pp.
464 21-35, 2017.
- 465 [15] A. Anees, Y.P.P. Chen, “True real time pricing and combined power scheduling of electric appliances
466 in residential energy management system,” *Applied Energy*, vol. 165, pp. 592-600, 2016.
- 467 [16] M. Honarmand, A. Zakariazadeh, S. Jadid, “Optimal scheduling of electric vehicles in an
468 intelligent parking lot considering vehicle-to-grid concept and battery condition,” *Energy*, vol. 65, pp.
469 572-579, Feb. 2014.

- 470 [17]S. Khemakhem, M. Rekik, L. Krichen, "A flexible control strategy of plug-
471 in electric vehicles operating in seven modes for smoothing load power curves in smart grid,"
472 *Energy*, vol. 118, pp. 197-208, Jan. 2017.
- 473 [18]B. Soares M. C. Borba, A. Szklo, R. Schaeffer, "Plug-in hybrid electric vehicles as a way to
474 maximize the integration of variable renewable energy in power systems: The case of wind
475 generation in northeastern Brazil," *Energy*, vol. 37, pp. 469-481, Jan. 2012.
- 476 [19] S. Tabatabaee, S. S. Mortazavi, T. Niknam, "Stochastic Scheduling of Local Distribution Systems
477 Considering High Penetration of Plug-in Electric Vehicles and Renewable Energy Sources," *Energy*,
478 (Article in press), 2017.
- 479 [20] K. M. Tan, V. K. Ramachandaramurthy, J. Y. Yong, "Optimal vehicle to grid planning and
480 scheduling using double layer multi-objective algorithm," *Energy*, vol. 112, pp. 1060-1073, Oct.
481 2016.
- 482 [21] M. Aziz, T. Oda, M. Ito, "Battery-assisted charging system for simultaneous charging
483 of electric vehicles," *Energy*, vol. 100, pp. 82-90, April 2016.
- 484 [22]L. Cheng, Y. Chang, and R. Huang, "Simulation tool for energy management of photovoltaic systems
485 in electric vehicles," *IEEE Transactions on Sustainable Energy*, vol.6, no.4, pp.1475-1484, 2015.
- 486 [23]A. Kavousi-Fard, T. Niknam, and M. Fotuhi-Firuzabad, "Stochastic reconfiguration and optimal
487 coordination of V2G plug-in electric vehicles considering correlated wind power generation," *IEEE*
488 *Transactions on Sustainable Energy*, vol.6, no.3, pp.822-830, 2015.
- 489 [24]S.F. Abdelsamad, W.G. Morsi, and T.S. Sidhu, "Impact of wind-based distributed generation on
490 electric energy in distribution systems embedded with electric vehicles," *IEEE Transactions on*
491 *Sustainable Energy*, vol.6, no.1, pp.79-87, 2015.
- 492 [25]C.X. Wu, C.Y. Chung, F.S. Wen, and D.Y. Du, "Reliability/cost evaluation with PEV and wind
493 generation system," *IEEE Transactions on Sustainable Energy*, vol.5, no.1, pp.273-281, 2014.
- 494 [26]I. Momber, G. Morales-Espana, A. Ramos, and T. Gomez, "PEV storage in multi-bus scheduling
495 problems," *IEEE Trans on Smart Grid.*, vol. 5, no.2, pp.1079-1087, March 2014.

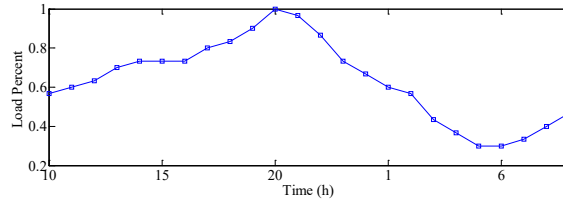
- 496 [27]H. Wang, S. Dusmez, and A. Khaligh, “Design and analysis of a full-bridge LLC-based PEV charger
497 optimized for wide battery voltage range,” *IEEE Transactions on Vehicular Technology*, vol.63, no.4,
498 pp.1603-1613, 2014.
- 499 [28]T. Tanaka, T. Sekiya, H. Tanaka, M. Okamoto, and E. Hiraki, “Smart charger for electric vehicles
500 with power-quality compensator on single-phase three-wire distribution feeders,” *IEEE Transactions*
501 *on Industry Applications*, vol.49, no.6, pp.2628-2635, 2013.
- 502 [29]R.J. Ferreira, L.M. Miranda R.E. Araujo, and J.P. Lopes, “A new bi-directional charger for vehicle-
503 to-grid integration,” in *Innovative Smart Grid Technologies (ISGT Europe), 2nd IEEE PES*
504 *International Conference and Exhibition on*, pp.1-5, 2011.
- 505 [30]L. Yanxia, and J. Jiuchun, “Harmonic-study of electric vehicle chargers,” *Proceedings of the Eighth*
506 *International Conference on Electrical Machines and Systems*. pp. 2404 – 2407, Sept. 2005.
- 507 [31]M.C. Kisacikoglu, B. Ozpineci, and L.M. Tolbert, “EV/PHEV bidirectional charger assessment for
508 V2G reactive power operation,” *IEEE Transactions on Power Electronics*, vol.28, no.12, pp.5717-
509 5727, 2013.
- 510 [32]M. Kesler, M.C. Kisacikoglu, and L.M. Tolbert, “Vehicle-to-Grid reactive power operation using
511 plug-in electric vehicle bidirectional offboard charger,” *IEEE Transactions on Industrial Electronics*,
512 vol.61, no.12, pp.6778-6784, 2014.
- 513 [33]M. C. B. P. Rodrigues, I. Souza, A. A. Ferreira, P. G. Barbosa, and H. A. C. Braga, “Integrated
514 bidirectional single-phase vehicle-to-grid interface with active power filter capability, ” *2013*
515 *Brazilian Power Electronics Conference*, pp. 993-1000, 2013.
- 516 [34]M.C. Kisacikoglu, M. Kesler, and L.M. Tolbert, “Single-phase on-board bidirectional PEV charger
517 for V2G reactive power operation,” *IEEE Trans. Smart Grid*, vol. 6, pp. 767-775, 2015.
- 518 [35]A. Ghosh, and G. Ledwich, Power quality enhancement using custom power devices, *Kluwer*
519 *Academic Publishers, USA*, 2002.
- 520 [36]N.G. Hingorani, and L. Gyugyi, Understanding FACTS, *IEEE Press, New York*, 1999.

- 521 [37]S. Biswas, S. Kumar, and A. Chatterjee, "Optimal distributed generation placement in shunt capacitor
522 compensated distribution systems considering voltage sag and harmonics distortions," *IET,
523 Generation, Transmission & Distribution*, vol.8, no.5, pp.783-797, 2014.
- 524 [38]K.L. Lian, and T. Noda, "Review of harmonic load flow formulations," *IEEE Transactions on Power
525 Delivery*, vol. 18, no. 3, pp. 1079-1087, July 2003.
- 526 [39]S. Herraiz, L. Sainz, and J. Clua, "A time-domain harmonic power flow algorithm for obtaining
527 nonsinusoidal steady state solutions," *IEEE Transactions on Power Delivery*, vol. 25, no. 3, pp. 1888-
528 1899, 2010.
- 529 [40]S. Pirouzi, M. A. Latify, and G. R. Yousefi, "Investigation on reactive power support capability of
530 PEVs in distribution network operation," in *Proc. 23rd Iran. Conf. Elect. Eng.*, pp. 1591–1596, May
531 2015.
- 532 [41]S. Pirouzi, J. Aghaei, M. Shafie-khah, G.J. Osório, J.P.S. Catalão, "Evaluating the security of
533 electrical energy distribution networks in the presence of electric vehicles," in *Proc. Power Tech Conf,
534 IEEE Manchester*, pp. 1-6, 2017.
- 535 [42]S. Pirouzi, J. Aghaei, V. Vahidinasab, T. Niknam, and A. Khodaei, "Robust linear architecture for
536 active/reactive power scheduling of EV integrated smart distribution networks," *Electric Power
537 System Research*, vol. 155, pp. 8-20, 2018.
- 538 [43]A. Rabiee, H. Farahani, M. Khalili, J.Aghaei, K. Muttaqi, "Integration of plug-
539 in electric vehicles into microgrids as energy and reactive power providers in market environment,"
540 *IEEE Transactions on Industrial Informatics*, DOI: 10.1109/TII.2016.2569438, *Article in press*,
541 2016.
- 542 [44]C.K. Duffey, and R. Stratford, "Update of harmonic standard IEEE-519: IEEE recommended
543 practices and requirements for harmonic control in electric power systems," *IEEE Transactions on
544 Industry Applications*, vol. 25, no. 6, pp. 1025-1034, 1989.
- 545 [45]A.J. Conejo, E. Castillo, R. Minguez, and R. Garcid-Bertrand, *Decomposition Techniques in
546 Mathematical Programming*, Springer, 2006.
- 547 [46]Generalized Algebraic Modeling Systems (GAMS). [Online]. Available: <http://www.gams.com>.

548 [47]A. Kavousi-Fard, and T. Niknam, "Optimal Distribution Feeder Reconfiguration for Reliability
549 Improvement Considering Uncertainty," *IEEE Trans. on Power Delivery*, vol. 29, no. 3, pp. 1344-
550 1354, 2014.

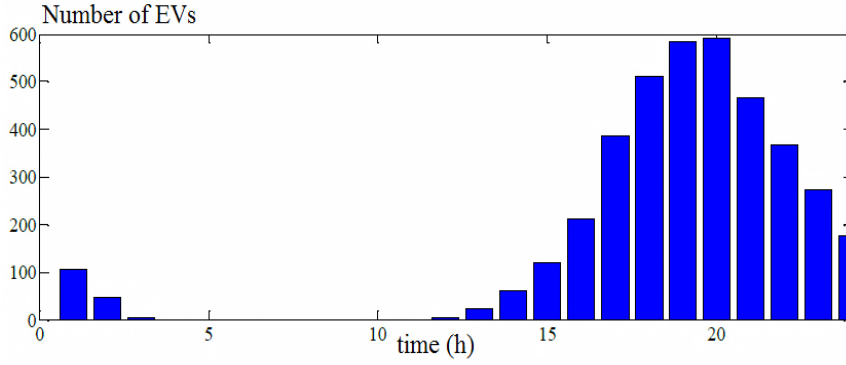
551 [48]Power Systems Test Case Archive, Univ. Washington [Online]. Available:
552 <http://www.ee.washington.edu/research/pstca>.

553



554

555 **Fig. 1.** Daily load percent curve [3].

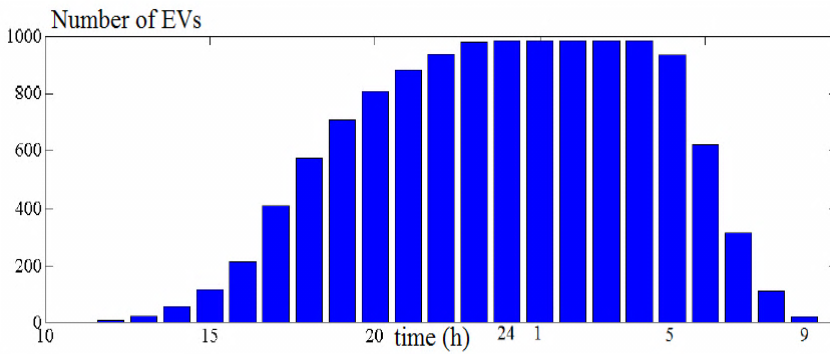


556

557

558

(a)



559

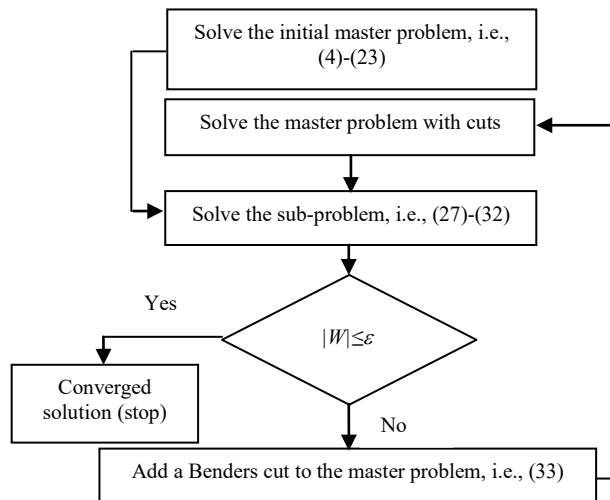
560

561

562

(b)

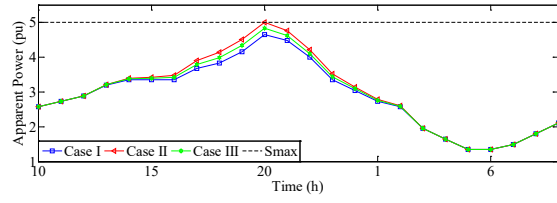
Fig. 2. The number of EVs at each hour, (a) Strategy I, (b) Strategy II.



563

564 **Fig. 3.** BD algorithm to solve the proposed problem.

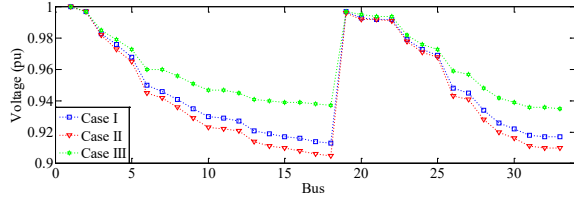
565



566

567

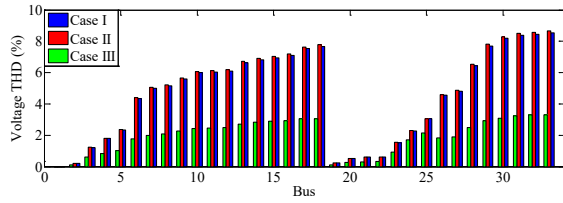
(a)



568

569

(b)



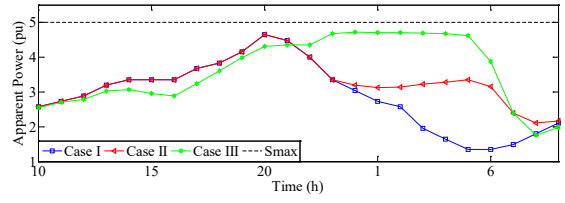
570

571

(c)

572 **Fig. 4.** Results of reactive power management and harmonic compensation using EVs based on Strategy
 573 I, (a), daily pattern of the network apparent power, (b) voltage profile at peak load time, and (c) voltage
 574 THD in each bus at peak load time.

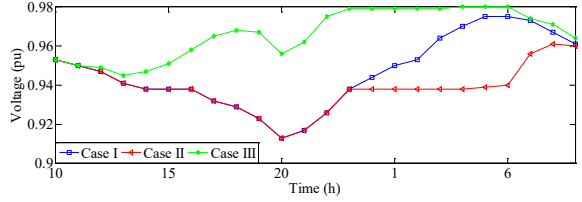
575



576

577

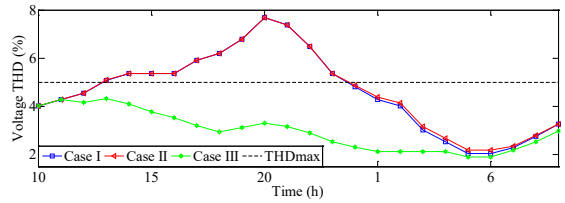
(a)



578

579

(b)



580

581

(c)

582 **Fig. 5.** Results of power management and harmonic compensation using EVs based on Strategy II, (a),
 583 daily pattern of the network apparent power, (b) daily pattern of the voltage in the bus 18, (c) daily pattern
 584 of the voltage THD in the bus 18.

585

586

Table 1 Taxonomy of recent works

Ref	Power management		Reactive	Harmonic compensation	Optimization problem	Solving with BD approach
	Active					
	Charging	Discharging				
[16]-[18]	Yes	No	No	No	Yes	No
[19]-[21]	Yes	Yes	No	No	Yes	No
[22]-[26]	Yes	Yes	No	No	Yes	No
[27]	Yes	No	No	Yes	No	No
[28]	Yes	No	Yes	Yes	No	No
[29]-[30]	Yes	No	No	Yes	No	No
Proposed model	Yes	No	Yes	Yes	Yes	Yes

587

588

Table 2 The value of active harmonic factor current [37]

h	1	5	7	11	13	17	19
HF^p	1	0.2	0.143	0.091	0.077	0.059	0.053
h	23	25	29	35	37	41	43
HF^p	0.043	0.04	0.034	0.029	0.027	0.024	0.015

589

590

Table 3 Characteristics of EV

Battery capacity (KWh) [1]	$BC \leq 8$	$8 < BC \leq 15$	$BC \geq 15$
State of charge [3]	0	0.15	0.25
Charger capacity (kVA) [1]	3.3	4.6	6.6
Charging time (h) [1]	≤ 4	2-4	≥ 2.5
Charge rate (kW) [1]	2	4	6
EVs in each group (%) [3]	20	60	20

591

592

Table 4 Buses with non-linear loads

Network	Bus no.
33-bus	4, 7, 10, 13, 18, 21, 25, 27, 30, 33
69-bus	4, 10, 16, 22, 27, 30, 35, 40, 46, 50, 55, 60, 65
123-bus	4, 6, 11, 12, 16, 20, 24, 29, 33, 39, 46, 59, 83, 90, 104

593

594

595

596

597

Table 5 Calculation time of problem solution with and without BD algorithm

Network (bus)		33-bus	69-bus	123-bus	
BD converged ($ W $ in pu)		0.03	0.10	0.15	
With BD algorithm		123	231	312	
Calculation time of (seconds)	without BD	CONOPT	981	Out of memory	Infeasible
	algorithm	BARON	993	Out of memory	Infeasible
		COUENNE	990	Out of memory	Infeasible
	(different solvers of GAMS software)	IPOPT	Infeasible	Infeasible	Infeasible
		KNITRO	978	Out of memory	Infeasible
		MINOS	994	Out of memory	Infeasible

598

599

Table 6 Number of variables and equations of problem with and without BD algorithm

Number of		Equations	Variables
without BD algorithm		58642	116424
With BD	Master problem	55474 with benders cut equation	116424
algorithm	Sub-problem	6337	69697

600

601